New Pnictinogallanes $[H_2GaE(SiMe_3)_2]_3$ (E = P, As)—Formation, Structural Characterization, and Thermal Decomposition to Afford Nanocrystalline GaP and GaAs

Jerzy F. Janik,[†,‡] Richard L. Wells,*[,‡] Victor G. Young, Jr.,[§] Arnold L. Rheingold,[⊥] and Ilia A. Guzei[⊥]

Contribution from the Department of Chemistry, Paul M. Gross Chemical Laboratory, Duke University, Durham, North Carolina 27708-0346, Department of Chemistry, X-ray Crystallographic Laboratory, University of Minnesota, Minneapolis, Minnesota 55455, and Department of Chemistry, University of Delaware, Newark, Delaware 19716

Received September 10, 1997

Abstract: The new compounds $[H_2GaE(SiMe_3)_2]_3$ (E = P **(1)**, As **(2)**), the first authenticated examples of a phosphinogallane and an arsinogallane containing the GaH_2 moiety, are prepared *via* efficient dehydrosilylation from the respective combinations of $H_3Ga{\cdot}NMe_3$ and $E(SiMe_3)_3$ in diethyl ether or toluene. Compounds **1** and **2** are characterized by elemental analysis, NMR, IR, and mass spectrometry. Single-crystal X-ray structural studies show that the molecular structures of **1** and **2** feature a flattened six-member ring of alternating Ga and E centers. Both compounds are reasonably stable at −30 °C but spontaneously decompose at ambient temperatures, **2** noticeably faster than **1**, with the evolution of $HSiMe_3$, H_2, and $E(SiMe_3)_3$. The pyrolysis of **1** yields nanocrystalline GaP while the pyrolysis of solids from decayed **2** results in nanocrystalline GaAs as determined from XRD studies. Under applied pyrolysis conditions, the thermally accelerated dehydrosilylation of the precursors is accompanied by a side-evolution of CH_4 and retention of small quantities of amorphous Si/C phases.

Introduction

Trimethylhalosilane elimination, or dehalosilylation, has proven to be a convenient route for making group 13(M)−15(E) element bonds from the starting materials MX_3 and $E(SiMe_3)_3$ and, in favorable cases, a removal of all ligands and formation of the solid-state ME materials has been achieved.[1] However, a complete elimination of redundant Me_3SiX groups is rare in standard bulk syntheses and residual, usually amorphous Si/C phases have been observed in the solid products in addition to the major crystalline ME.[1e,2] On one hand, this phenomenon results in composite materials with potentially useful properties but, on the other hand, it poses an outstanding challenge with regard to separation of such phases, if necessary. Interestingly, if one uses a related group 13−15 substituent isomer system, e.g. $\{Al(SiMe_3)_3\} + PCl_3$ (or R_2PCl), the prevailing reaction pathway under ambient conditions is not dehalosilylation as defined above but ligand exchange with subsequent P−P coupling side reactions.[3]

We have recently reported on the high yield syntheses and structural characterizations of the novel lithium pnictidogallates, $(Et_2O)_2Li[\mu\text{-}E(SiMe_3)_2]_2GaH_2$, E = P, As, that were obtained from the respective combinations of $LiGaH_4$ and $E(SiMe_3)_3$ in Et_2O *via* facile dehydrosilylation.[4] Under specific reaction conditions for E = P, we observed the formation of a minor byproduct whose spectroscopic characterization was consistent with the building blocks of $\{H_2GaP(SiMe_3)_2\}$. There have also been other precedences for the trimethylsilane elimination-condensation reactions in related group 13−15 systems, examples of which include $\{BH_3\}/P(SiMe_3)_3$,[5] $\{Al(SiMe_3)_3\}/$

* Address correspondence to R. L. Wells.
† On leave from the University of Mining and Metallurgy, Krakow, Poland.
‡ Duke University.
§ University of Minnesota.
⊥ University of Delaware.

(1) See for example: (a) Wells, R. L. *Coord. Chem. Rev.* **1992**, *112*, 273 (and references therein). (b) Aubuchon, S. R.; McPhail, A. T.; Wells, R. L.; Giambria, J. A. *Chem. Mater.* **1994**, *6*, 82. (c) Wells, R. L.; Aubuchon, S. R.; Kher, S. S.; Lube, M. S.; White, P. S. *Chem. Mater.* **1995**, *7*, 793. (d) Halaoui, L. I.; Kher, S. S.; Lube, M. S.; Aubuchon, S. R.; Hagan, C. R. S.; Wells, R. L.; Coury, L. A. *ACS Symp. Ser.* **1996**, *622*, 178 (and references therein). (e) Janik, J. F.; Baldwin, R. A.; Wells, R. L.; Pennington, W. T.; Schimek, G. L.; Rheingold, A. L.; Liable-Sands, L. M. *Organometallics* **1996**, *15*, 5385. (f) Wells, R. L.; Gladfelter, W. L. *J. Cluster Sci.* **1997**, *8*, 217 (and references therein). (g) Healy, M. D.; Laibinis, P. E.; Stupik, P. D.; Barron, A. R. *J. Chem. Soc., Chem. Commun.* **1989**, 359. (h) Olshavsky, M. A.; Goldstein, A. N.; Alivisatos, A. P. *J. Am. Chem. Soc.* **1990**, *112*, 9438. (i) Butler, L.; Redmond, G.; Fitzmaurice, D. *J. Phys. Chem.* **1993**, *97*, 10750. (j) Laurich, B. K.; Smith, D. C.; Healy, M. D. *Mater. Res. Soc. Symp. Proc.* **1994**, *351*, 49. (k) Micic, O. I.; Sprague, J. R.; Curtis, C. J.; Jones, K. M.; Machol, J. L.; Nozik, A. J.; Giessen, H.; Fluegel, B.; Mohs, G.; Peyghambarian, N. *J. Phys. Chem.* **1995**, *99*, 7754. (l) Guzelian, A. A.; Katari, J. E. B.; Kadavanich, A. V.; Banin, U.; Hamad, K.; Juban, E.; Alivisatos, A. P.; Wolters, R. H.; Arnold, C. C.; Heath, J. R. *J. Phys. Chem.* **1996**, *100*, 7212.

(2) (a) Paine, R. T.; Janik, J. F.; Fan, M. *Polyhedron* **1994**, *13*, 1225. (b) Sauls, F. C.; Hurley, W. J.; Interrante, L. V.; Marchetti, P. S.; Maciel, G. E. *Chem. Mater.* **1995**, *7*, 1361. (c) Paciorek, K. J. L.; Nakahara, J. H.; Hoferkamp, L. A.; George, C.; Flippen-Anderson, J. L.; Gilardi, R.; Schmidt, W. R. *Chem. Mater.* **1991**, *3*, 82. (d) Bender, B. A.; Rice, R.; Spann, J. R. L. *Ceram. Eng. Sci. Proc.* **1985**, *6*, 1171. (e) Izaki, K.; Hakkei, K.; Kawakami, T.; Niimara, K. *Ultrastructure Processing of Advanced Materials*; MacKenzie, J. D., Ulrich, D. R., Eds.; Wiley: New York, 1988; p 891. (f) Baixia, L.; Yinkui, L.; Yi, L. *J. Mater. Chem.* **1993**, *3*, 117.

(3) Janik, J. F.; Duesler, E. N.; McNamara, W. F.; Westerhausen, M.; Paine, R. T. *Organometallics* **1989**, *8*, 506.

(4) Janik, J. F.; Wells, R. L.; Young, V. G., Jr.; Halfen, J. A. *Organometallics* **1997**, *16*, 3022.

(5) Wood, G. L.; Dou, D.; Narula, C. K.; Duesler, E. N.; Paine, R. T.; Nöth, H. *Chem. Ber.* **1990**, *123*, 1455 (and references therein).

S0002-7863(97)03183-1 CCC: $15.00
Published on Web 01/13/1998

$PH_{3-n}R_n$,[3] and $\{Al(SiMe_3)_3\}/NH_3$[6] combinations. These observations and reports turned our attention toward investigating the $\{GaH_3\}/E(SiMe_3)_3$ reaction systems as a potential source for new molecular and polymeric precursors to GaE materials. The thermal instability of the Ga−H bond[7] was expected to enhance the elimination-condensation reactivity but also could lead to some undesirable side-decomposition pathways for these precursors.

Results and Discussion

The combinations of $H_3Ga{\cdot}NMe_3$ and $E(SiMe_3)_3$ in diethyl ether (preferably) or toluene at ambient conditions afforded $[H_2GaE(SiMe_3)_2]_3$, E = P **(1)**, As **(2)**, the first reported phosphinogallane and arsinogallane containing the GaH_2 moiety, as well as their elimination-condensation polymeric products, *via* very efficient dehydrosilylation (eq 1).

$$H_3Ga{\cdot}NMe_3 + E(SiMe_3)_3 \rightarrow {}^1/_3[H_2GaE(SiMe_3)_2]_3 + HSiMe_3 + NMe_3 \quad (1)$$

No reaction was detected for E = N under comparable conditions. This was in accord with a decreased reactivity of the N−$SiMe_3$ groups toward dehydrosilylation at ambient conditions due to the strong N−Si bond and steric congestion in $N(SiMe_3)_3$, as previously observed in the system $LiGaH_4/E(SiMe_3)_3$ (E = N, P, As).[4] Crystalline compounds **1** and **2** were obtained from the reaction mixtures in Et_2O at early stages of the reactions, and after isolation they seemed to be reasonably stable for several days to weeks if stored at −30 °C. If any of the compounds was left in the mother liquor it would further react and turn to a colored, insoluble polymeric solid. The NMR studies for samples prepared in toluene-d_8 from crystalline **1** and **2** as well as from their respective yellow to orange decomposition products showed amounts of byproducts such as $HSiMe_3$, H_2, and $E(SiMe_3)_3$ (especially for E = As) increasing with time. The occurrence of $HSiMe_3$ was consistent with progressing facile dehydrosilylation, the target elimination-condensation route in this study. However, the presence of the remaining byproducts indicated other decomposition pathways as well. The dihydrogen most likely resulted from a known reductive decomposition of gallanes, whereas the resultant $E(SiMe_3)_3$ were derived from a complex ligand redistribution chemistry operating in these systems. Interestingly, the same decomposition species were also observed by us in the related case of the lithium pnictidogallates, $(Et_2O)_2Li[\mu\text{-}E(SiMe_3)_2]_2\text{-}GaH_2$, E = P, As.[4] It appeared that in the presently investigated systems the decay of the molecular species was faster in toluene than in Et_2O. Also, the E = P system decomposed slower than the E = As system under analogous conditions, which resulted in a higher yield of the isolated P analogue; however, the yields of **1** and **2** were not optimized.

The elemental analysis and spectroscopic characterization of **1** indicated a product of $\{H_2GaP(SiMe_3)_2\}$ stoichiometry. In this regard, the infrared Ga−H stretching frequency at 1837 cm^{-1} was characteristic of terminal GaH_2 moieties.[8,9] The ^1H NMR spectrum obtained at 400 MHz consisted of an atypical, significantly broadened doublet for the $SiMe_3$ protons at δ 0.45 and a characteristic broad resonance for the GaH_2 protons[4] at δ 4.55 that integrated 9 to 1 as expected. Similarly, the $^{13}C\{^1H\}$ NMR spectrum showed four regularly spaced peaks that could be interpreted either as two closely spaced doublets or a second-order pattern. The rather unusual appearance of the proton doublet prompted us to run the sample at a higher field of 600 MHz with the hope to better resolve the possibly overlapped resonances. Under this condition, the resonance pattern and position for the $SiMe_3$ protons remained unchanged but the separation of the peaks in the apparent doublet decreased slightly. If the doublet resulted from a simple coupling of one phosphorus with one proton, the separation should have remained the same; we thus concluded that we dealt with complex and likely superimposed signals. On the basis of the above, we first ruled out a planar, dimeric structure for **1** (triplet expected for the $SiMe_3$ protons) and, for instance, a low symmetry trimer of the $\{H_2GaP(SiMe_3)_2\}$ species became probable. The singlet in the ^{31}P NMR spectrum at δ −265.8 was not of much help here but, in the related case of the trimer $[H_2BP(SiMe_3)_2]_3$,[5] a single phosphorus resonance was also observed. A strong argument for the trimeric oligomerization, at least in the evaporated state, was obtained from the mass spectrum of **1**. It clearly showed the highest *m*/*e* signal for the trimeric parent ion and other logical fragmentation signals.

Similarly as for **1**, the elemental analysis for compound **2** was consistent with the $\{H_2GaAs(SiMe_3)_2\}$ stoichiometry. On the other hand, the compound's spectroscopic characterization appeared to be simpler than that for **1**. For example, the ^1H and $^{13}C\{^1H\}$ NMR showed only sharp singlets for the $SiMe_3$ groups, indicating their symmetrical local environment in the solution. The proton resonance for the GaH_2 moieties at δ 4.65 was broad and featureless, and integrated as expected with the $SiMe_3$ proton signal. The infrared Ga−H stretch at 1834 cm^{-1} also supported the presence of the GaH_2 moieties in the molecule. And last, the mass spectrum showed a parent ion and a clean fragmentation pattern for the trimer $[H_2GaAs(SiMe_3)_2]_3$. Summarizing these observations, all the characterization data for **1** and **2** were consistent with the trimeric connectivities, but they also suggested some differences in the symmetry of the two rings, especially in solution. A convincing proof of the compounds' solid-state structures as trimers was provided by the single-crystal X-ray diffraction studies.

The trimer $[H_2GaP(SiMe_3)_2]_3$ **(1)** appears to be the first published example of a phosphinogallane containing the GaH_2 group. It features a six-membered ring of alternating Ga and P centers as shown in Figure 1. Curiously, the thermal parameters for the Ga atom are about twice the magnitude of the P atom, yet both atoms occupy structurally similar positions, i.e., both are members of the ring. In fact, the value for Ga is similar to that of the Si atom which is in an inherently more thermally active side-chain position. Interestingly, unusually thermally active group 13 atoms are also found in two related ring systems: in $[H_2GaAs(SiMe_3)_2]_3$ in which P is replaced by As (*vide infra*), and in $[H_2BP(SiMe_3)_2]_3$[5] in which Ga is replaced by B. On the basis of crystallographic constraints for **1**, the hexagonal site symmetry imposes strict mirror-plane symmetry on the ring atoms. However, the molecular symmetry of **1** may be lower than the crystallographic site symmetry. Another factor contributing to ring puckering can stem from inherent differ-

(6) (a) Janik, J. F.; Duesler, E. N.; Paine, R. T. *Inorg. Chem.* **1987**, *26*, 4341. (b) Janik, J. F.; Duesler, E. N.; Paine, R. T. *Inorg. Chem.* **1988**, *27*, 4335.

(7) See for example: (a) Downs, A. J., Ed. *Chemistry of Aluminium, Gallium, Indium and Thallium*, Blackie-Chapman Hall: London, 1993. (b) Jones, C.; Kousantonis, G. A.; Raston, C. L. *Polyhedron* **1993**, *12*, 1829.

(8) Pulham, C. R.; Downs, A. J.; Goode, M. J.; Rankin, D. W. H.; Robertson, H. E. *J. Am. Chem. Soc.* **1991**, *113*, 5149 (and references therein).

(9) (a) Pulham, C. R.; Downs, A. J.; Rankin, D. W. H.; Robertson, H. E. *J. Chem. Soc., Dalton Trans.* **1992**, 1509. (b) Henderson, M. J.; Kennard, C. H. L.; Raston, C. L.; Smith, G. *J. Chem. Soc., Chem. Commun.* **1990**, 1203. (c) Baxter, P. L.; Downs, A. J.; Rankin, D. W. H.; Robertson, H. E. *J. Chem. Soc., Dalton Trans.* **1985**, 807. (d) Hwang, J.-W.; Hanson, S. A.; Britton, D.; Evans, J. F.; Jensen, K. F.; Gladfelter, W. L. *Chem. Mater.* **1990**, *2*, 342.

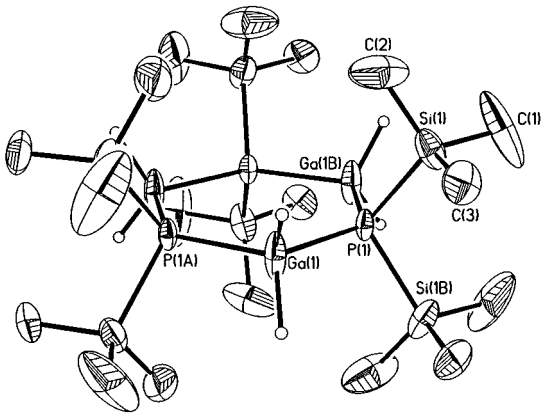

Figure 1. Thermal ellipsoid diagram (35% probability ellipsoids) showing the molecular structure of **1**. All carbon−hydrogen atoms are omitted for clarity.

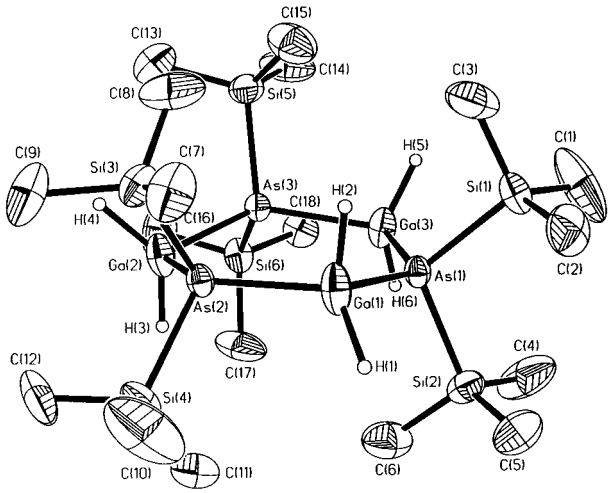

Figure 2. Thermal ellipsoid diagram (35% probability ellipsoids) showing the molecular structure of **2**. All carbon−hydrogen atoms are omitted for clarity.

ences in bonding of Ga and P atoms in the ring which result in the Ga atoms that have greater librational freedom or, alternatively, more rigid P atoms can accommodate more ring strain compared to their neighbors. We calculated librational corrections for the vibrationally averaged positions, which led to an increase in the average Ga−P distance of only 0.006 Å. However, even this small change indicates that the ring is probably not planar, in accord with the analogous structures.

The ring angles in **1** illustrate some of the points discussed above. The Ga−P−Ga angles of 126.35(10)° are significantly larger than the neighboring P−Ga−P angles of 113.65(10)°. Alternatively, this can be rationalized in terms of a greater ring strain at the P centers (rigidity) than at the Ga centers (librational freedom). A few related and structurally characterized (or calculated) organophosphine gallane adducts $H_3Ga{\cdot}PR_3$ with four-coordinated Ga and P atoms, and typical dative bonds, provide the following Ga−P bond lengths: $H_3Ga{\cdot}P(C_6H_{11})_3$,[10a] 2.460(2) Å; $(H_3Ga)_2{\cdot}(PMe_2CH_2)_2$,[10a] 2.399(4) Å; $H_3Ga{\cdot}PH_3$ (calculated),[10a] 2.576 Å; $H_3Ga{\cdot}P(t\text{-}Bu)_3$,[10b] 2.444(6) Å; $H_3Ga{\cdot}PMe_3$ (calculated),[10b] 2.550 Å. The average Ga−P length in **1** of 2.392 Å is, however, more appropriately compared with the Ga−P distances found in the planar dimers exemplified by $[Cl_2GaP(SiMe_3)_2]_2$,[11a] av 2.379 Å, $[Br_2GaP(SiMe_3)_2]_2$,[11b] av 2.386 Å, $[I_2GaP(SiMe_3)_2]_2$,[11c] av 2.397 Å, $[Me_2GaP(SiMe_3)_2]_2$,[11d] 2.456(1) Å, and $(Et_2O)_2Li[\mu\text{-}P(SiMe_3)_2]_2GaH_2$,[4] 2.4122(12) Å or in the trimers such as planar $[t\text{-}Bu_2GaPH_2]_3$,[12a] 2.439(3) Å, boat $[Me_2GaP(i\text{-}Pr)_2]_3$,[12b] av 2.442 Å, or chair $[Me_2GaP(Me)Ph]_3$,[12c] av 2.410 Å.

The molecular structure of $[H_2GaAs(SiMe_3)_2]_3$ **(2)** in the solid state, the first reported arsinogallane containing the GaH_2 moiety, is shown in Figure 2. It confirms a trimeric core of alternating four-coordinated Ga and As centers. The ring has an apparent twist boat conformation but displays a significant flattening wherein the ligands assume a close to symmetrical arrangement above and below the core. Such a ligand configuration could be partly responsible for the observed equivalency of the $SiMe_3$ protons and carbons in the NMR spectra. The ring flattening, with maximum displacement from planarity of 0.25 Å, is demonstrated by the close and small values of the Ga−As−Ga−As torsion angles listed in Table 2. It also has some impact on the ring internal angles and associated ligand strain. The As−Ga−As average angle, 110.95°, is smaller than the average Ga−As−Ga angle, 127.08°, indicating significant strain at the As centers in accord with what was discussed above for **1**. This, however, seems to be compensated by the smaller Si−As−Si angles (av 107.53°) than the H−Ga−H angles (av 127°), an apparent benefit of the small H ligand size. A similarly flattened ring was earlier reported for the related borane derivative, $[H_2BP(SiMe_3)_2]_3$,[5] in a twist chair conformation. The Ga−As average bond length in **2**, 2.4742 Å, is rather short among the relevant four-coordinated Ga−As compounds and can be compared with the bond distances in the related $(Et_2O)_2Li[\mu\text{-}As(SiMe_3)_2]_2GaH_2$,[4] 2.4941(5) Å, $[I_2GaAs(SiMe_3)_2]_2$,[13a] av 2.471 Å, or $[(Me_3SiCH_2)_2GaAs(SiMe_3)_2]_2$,[13b] av 2.567 Å. Also, the Ga−H average bond length, 1.50(3) Å, compares well with the Ga−H distances in the closely related $(Et_2O)_2Li[\mu\text{-}E(SiMe_3)_2]_2GaH_2$,[4] where for E = P it was 1.58(4) Å and for E = As it showed 1.51(5) Å. Generally, this value is in the typical range for terminal Ga−H bond lengths as illustrated by the following cases: Ga_2H_6 (gas phase),[14] 1.519(35) Å for the terminal hydrogens (1.710(38) Å for the bridging hydrogens); $[Me_2NGaH_2]_2$ (gas phase),[9c] 1.487(36) Å; a solid product from the reaction between $H_3Ga{\cdot}NMe_3$ and 1,4-di-*tert*-butyl-1,4-diazabutadiene[9b] containing a terminal GaH_2 group, 1.57(8) Å and 1.54(12) Å.

Theoretically, decomposition of the trimers, $[H_2GaE(SiMe_3)_2]_3$, *via* dehydrosilylation should result in the GaE binaries that, noting the efficiency of the $HSiMe_3$ elimination at ambient conditions, should take place at relatively low temperatures compared with other precursor routes, especially for E = P. In this regard, the relevant $X_3Ga/P(SiMe_3)_3$[1a,b,e,f] (*X* = halide) dehalosilylation systems were earlier reported to form stable

(10) (a) Atwood, J. L.; Robinson, K. D.; Bennett, F. R.; Elms, F. M.; Koutsantonis, G. A.; Raston, C. L.; Young, D. J. *Inorg. Chem.* **1992**, *31*, 2673. (b) Elms, F. M.; Gardiner, M. G.; Koutsantonis, G. A.; Raston, C. L.; Atwood, J. L.; Robinson, K. D. *J. Organomet. Chem.* **1993**, *449*, 45.

(11) (a) Wells, R. L.; Self, M. F.; McPhail, A. T.; Aubuchon, S. R.; Woudenberg, R. C.; Jasinski, J. P. *Organometallics* **1993**, *12*, 2832. (b) Aubuchon, S. R.; McPhail, A. T.; Wells, R. T.; Giambria, J. A.; Bowser, J. R. *Chem. Mater.* **1994**, *6*, 82. (c) Aubuchon, S. R.; Lube, M. S.; Wells, R. L. *Chem. Vap. Deposition* **1995**, *1*, 1. (d) Dillingham, M. D. B.; Burns, J. A.; Byers-Hill, J.; Gripper, K. D.; Robinson, G. H. *Inorg. Chim. Acta* **1994**, *216*, 267.

(12) (a) Cowley, A. H.; Harris, P. R.; Jones, R. A.; Nunn, C. M. *Organometallics* **1991**, *10*, 652. (b) Cowley, A. H.; Jones, R. A.; Mardones, M. A.; Nunn, C. M. *Organometallics* **1991**, *10*, 1635. (c) Beachley, O. T., Jr.; Royster, T. L.; Arhar, J. R.; Rheingold, A. L. *Organometallics* **1993**, *12*, 1976.

(13) (a) Johansen, J. D.; McPhail, A. T.; Wells, R. L. *Adv. Mater. Opt. Electron.* **1992**, *1*, 29. (b) Wells, R. L.; Pasterczyk, J. W.; McPhail, A. T.; Johansen, J. D.; Alvanipour, A. *J. Organomet. Chem.* **1991**, *407*, 17.

(14) Pulham, C. R.; Downs, A. J.; Goode, M. J.; Rankin, D. W. H.; Robertson, H. E. *J. Am. Chem. Soc.* **1991**, *113*, 5149.

adducts at room temperature and only prolonged sonication or reflux in hexane caused a removal of one Me_3SiX equivalent and the formation of $[X_2GaP(SiMe_3)_2]_2$. The pyrolyses of these adducts at 450 °C under vacuum resulted in the formation of mostly nanocrystalline GaP but also in retention of some Si/C phases from thermal cracking of residual $SiMe_3$ groups.[1e] On the other hand, the $X_3Ga/As(SiMe_3)_3$[1a,f,h,i] dehalosilylation system was found for X = Cl to eliminate at room temperature approximately 2 equiv of Me_3SiCl, but for X = Br, I only 1 equiv of Me_3SiX was observed. The pyrolyses of these precursors yielded GaAs solids apparently containing none or very little Si/C residues.

In the present study, the pyrolyses of the precursors from the $\{GaH_3\}/P(SiMe_3)_3$ system, compound **1** and the related colored polymeric solid, under applied conditions afforded nanocrystalline GaP with the average crystallite size of 2.3 (450 °C, vacuum) or 29.4 nm (600 °C, vacuum), and 5.1 nm (475 °C, vacuum), respectively. However, a mismatch between the theoretical and observed TGA weight losses, the presence of CH_4 in the pyrolysis off-gases, and the elemental analysis of the pyrolysates all clearly indicated an incomplete $HSiMe_3$ elimination and the resulting cracking of the $SiMe_3$ groups that eventually led to the retention of Si/C amorphous phases in the final product. Additionally, the detection of the $P(SiMe_3)_3$ byproduct pointed to other decomposition side reactions as well. Interestingly, the analyzed silicon and carbon contents were similar to those observed for some of the pyrolysis products from the $X_3Ga/P(SiMe_3)_3$ dehalosilylation systems.[1e] Regarding the $\{GaH_3\}/As(SiMe_3)_3$ system, the pyrolysis of pure compound **2** was not possible due to its fast decomposition at ambient conditions. However, the reflux in xylenes (bp 137−144 °C) of the colored polymeric solid obtained in this system resulted in a product with an XRD spectrum that indicated the onset of GaAs crystallinity. The pyrolysis of the polymeric solid at 450 °C under vacuum yielded nanocrystalline GaAs with the average crystallite size of 3.4 nm as determined by XRD. Similarly with the analogous phosphorus system, the analytical evidence supported the retention of the Si/C species in the final product. Additionally, there appeared to be a significant excess of gallium, i.e., Ga/As was found at 1.5/1.0. This feature was a likely consequence of the low barrier decomposition of the precursors along the $E(SiMe_3)_3$ and H_2 elimination pathways which were much more acute for E = As than for E = P. These pathways would have been expected to lead to some gallium rich phase due to arsenic depletion (decay of GaH_2 moieties associated with H_2 evolution plus the formation and removal of the soluble $As(SiMe_3)_3$ byproduct). It should be stressed, however, that the major crystalline product by XRD was the nanosized GaAs and both the minor gallium rich and Si/C byproducts seemed to be separate. In summary, the facile $HSiMe_3$ elimination-condensation chemistry for these precursors was found to coexist and compete with other decomposition pathways associated with the inherent fragility of the Ga−H bonds.

Experimental Section

General Techniques. All experiments were performed with standard vacuum/Schlenk techniques. Solvents were distilled from sodium benzophenone ketyl or Na/K alloy prior to use. $H_3Ga{\cdot}NMe_3$,[15] $P(SiMe_3)_3$,[16] and $As(SiMe_3)_3$[17] were prepared by literature methods. $N(SiMe_3)_3$ was obtained from Aldrich and used as received. ^1H, $^{13}C\{^1H\}$, and ^{31}P NMR spectra were recorded on the Varian Unity 400 and Unity 600 spectrometers at 25 °C from toluene-d_8 solutions and referenced *vs* $SiMe_4$ by generally accepted methods. Mass spectra were collected on a JEOL JMS-SX 102A spectrometer operating in the EI mode at 20 eV; the assignment of the ion fragments was supported by comparison with theoretical ion distributions. IR spectra of solids and gaseous pyrolysis products were acquired by use of KBr pellets and a gas cell, respectively, on a BOMEM Michelson MB-100 FT-IR spectrometer. A calibrated manifold was used for volume estimations of reaction gases. TGA/DTA analyses were acquired under an UHP nitrogen flow on a TA Instruments SDT 2960 simultaneous TGA/DTA apparatus. Elemental analyses were provided by E + R Microanalytical Laboratory, Corona, NY. Melting points (uncorrected) were determined with a Thomas-Hoover Uni-melt apparatus for samples flame sealed in glass capillaries. Single-crystal X-ray diffraction study for **1** was performed at the University of Delaware, Department of Chemistry and Biochemistry, Newark, DE, on a Siemens P4 diffractometer, and study for **2** was carried out at the University of Minnesota, X-ray Crystallographic Laboratory, Minneapolis, MN, on a Siemens SMART Platform CCD system with in both cases Mo Kα radiation (λ = 0.71073 Å) at 203(2) K for **1** and at 173(2) K for **2**. All calculations were carried out with the SHELXTL V5.0 or V5.03 suite of programs;[18] the structures were solved by direct methods. XRD data were collected by using mineral oil coated samples on a Phillips XRD 3000 diffractometer utilizing Cu Kα radiation; the average particle sizes of GaP and GaAs pyrolysis products were calculated by using the Scherrer equation applied to the (111) diffraction lines of the cubic GaP and GaAs.

Reaction System $H_3Ga{\cdot}NMe_3/P(SiMe_3)_3$. (1) Synthesis of $[H_2GaP(SiMe_3)_2]_3$ (1) in Et_2O. A sample of freshly prepared $H_3Ga{\cdot}NMe_3$ (0.40 g, 3.0 mmol) was dissolved in 30 mL of Et_2O. To this was added a solution of $P(SiMe_3)_3$ (0.75 g, 3.0 mmol) in 15 mL of Et_2O at room temperature. After being stirred overnight, the solution was partially evacuated to 5−10 mL and stored at −30 °C, which resulted in the formation of small colorless crystals. The crystals were separated from the mother liquor and evacuated for 10 min (0.48 g). After the mother liquor was further concentrated to less than 5 mL, another batch of crystals was obtained at −30 °C (0.10 g). Total yield, 0.58 g or 78% based on eq 1 (vide infra). Storage of solid **1** at room temperature for several hours to days resulted in a gradual color change to yellow. X-ray quality crystals were first obtained at −30 °C from both the ethereal and toluene solutions of **1**; however, serious twinning problems prevented a satisfactory crystallographic refinement. Crystals of **1** of better quality were eventually obtained from a related reaction system in which **1** appeared to be a major byproduct.[19] Melting behavior: 150−160 °C, change of color to brown-black; no melting to 300 °C. Anal. Found (calcd) for $C_{18}H_{60}Ga_3P_3Si_6$: C, 28.72 (28.93); H, 7.85 (8.09). ^1H NMR (400 MHz): δ 0.45 (54H, $SiMe_3$; high-neck doublet, apparent J_{P-H} coupling of 4.6 Hz), 4.55 (6H, GaH_2, br). ^1H NMR (600 MHz): δ 0.45 (54H, $SiMe_3$; high-neck doublet, apparent J_{P-H} coupling of 3.6 Hz), 4.54 (6H, GaH_2). $^{13}C\{^1H\}$ NMR (400 MHz) (intensity): δ 1.982 (80), 1.955 (100), 1.929 (100), 1.902 (80). ^{13}C NMR (600 MHz) (intensity): δ 1.998 (85), 1.979 (100), 1.965 (80), 1.946 (90). $^{31}P\{^1H\}$ NMR (400 MHz): δ −265.8. MS: *m/e* (intensity)(ion): peak clusters around 746 (3)($[H_2GaP(SiMe_3)_2]_3$ or M), 731 (1)(M − Me), 673 (1)(M − $SiMe_3$), 568 (25)(M − $P(SiMe_3)_2$), 496 (100)($[H_2GaP(SiMe_3)_2]_2$ − 2H or M^* − 2H), 483 (2)(M^* − Me), 425 (13)(M^* − $SiMe_3$), 409 (2)(M^* − $SiMe_3$ − Me − H), 318 (12)(M^* − $P(SiMe_3)_2$ − 3H), 247 (40)($H_2GaP(SiMe_3)_2$ − H or M^{**} − H; possible contribution from $P(SiMe_3)_3$ at *m/e* 250), 235 (2)($P(SiMe_3)_3$ − Me), 178 (28)($HP(SiMe_3)_2$), 163 (11)($HP(SiMe_3)_2$ − Me), 147 (15)($P(SiMe_3)_2$ − 2Me), 73 (26)($SiMe_3$), 59 (2)($HSiMe_2$). IR: ν(Ga−H) 1837 cm^{-1}.

(15) Shirk, A. E.; Shriver, D. F. *Inorg. Synth.* **1977**, *17*, 42.
(16) Becker, G.; Hölderich, W. *Chem. Ber.* **1975**, *108*, 2484.
(17) (a) Becker, G.; Gutenkunst, G.; Wessely, H. J. *Z. Anorg. Allg. Chem.* **1980**, *462*, 113. (b) Wells, R. L.; Self, M. S.; Johansen, J. D.; Laske, J. A.; Aubuchon, S. R.; Jones, L. J. *Inorg. Synth.* **1997**, *31*, 150.
(18) SHELXTL-plus V5.03 **(1)** or V5.0 **(2)**, Siemens Industrial Automation, Inc., Madison, WI.
(19) The reactions of $(Et_2O)_2Li[\mu\text{-}P(SiMe_3)_2]GaH_2$ with some compounds of the type R_nMX_{3-n} (M = group 13 element; R = H, alkyl, aryl; X = halogen; n = 0, 1, 2), performed in our laboratory, have yielded $[H_2GaP(SiMe_3)_2]_3$ as a major byproduct. X-ray quality crystals of the trimer were obtained from the reaction between $(Et_2O)_2Li[\mu\text{-}P(SiMe_3)_2]GaH_2$ and Me_2BBr in toluene (Wells, R. L.; Jouette, J. R.; Janik, J. F. To be submitted for publication).

Table 1. Crystallographic Data and Measurements for **1** and **2**

	1	**2**
molecular formula	$C_{18}H_{60}Ga_3P_3Si_6$	$C_{18}H_{60}Ga_3As_3Si_6$
formula weight	747.27	879.12
crystal system	hexagonal	monoclinic
space group	$P6_3/m$	$P2_1/n$
a, Å	11.8477(2)	11.9593(2)
b, Å	11.8477(2)	16.7702(3)
c, Å	16.7845(4)	20.3940(4)
β, deg	90	90.3640(10)
V, Å^3	2040.36(7)	4090.14(13)
Z	2	4
radiation (wavelength, Å)	Mo Kα (0.71073)	Mo Kα (0.71073)
μ, mm^{-1}	2.268	4.554
temp, K	203(2)	173(2)
D_{calcd}, g/cm^3	1.216	1.428
crystal dimens, mm	0.4 × 0.4 × 0.4	0.38 × 0.35 × 0.30
T_{max}/T_{min}	1.00/0.50	1.0000/0.7527
Θ range for data collection, deg	1.98−28.28	1.57−25.02
no. of reflcns collected	7582	20340
no. of independent reflcns	1681 (R_{int} = 0.0371)	7149 (R_{int} = 0.0334)
data/restraints/parameters	1673/0/53	7149/15/295
R1 ($I>2\sigma(I)$);[a] wR2[b]	0.0893; 0.1989	0.0503; 0.0866
R1 (all data);[a] wR2[b]	0.1102; 0.2254	0.0801; 0.0943
goodness of fit[c]	1.127	1.096
final max/min $\Delta\rho$, e/Å^{-3}	0.879/−0.926	0.903/−0.763

[a] $R_{int} = \sum|F_o^2 - \langle F_o\rangle^2|/\sum|F_o^2|$; $R1 = \sum||F_o| - |F_c||/\sum|F_o|$. [b] $wR2 = [\sum[w(F_o^2 - F_c^2)^2]/\sum[w(F_o^2)^2]]^{1/2}$ where $w = 1/\sigma^2(F_o^2) + (aP)^2 + bP$. [c] GooF $= S = [\sum[w(F_o^2 - F_c^2)^2]/(n-p)^{1/2}$.

(2) Reaction of $H_3Ga{\cdot}NMe_3$ with $P(SiMe_3)_3$ in Toluene. The reaction in toluene was performed similarly as above. After 2 days at room temperature, the mixture turned yellow and, after an additional 2 days at −30 °C, orange. At the end of the fourth day, the volatiles were removed and the resulting orange solid was evacuated for 3 h. The solid could not be redissolved in fresh toluene afterward. A ^{1}H NMR study of the toluene-d_8 slurry of the orange solid showed abundant $P(SiMe_3)_3$, some $HSiMe_3$, H_2,[8] and a very broad peak feature at δ 0.6; no discernible Ga−H resonances were observed between δ 4 and 6. IR: ν(Ga−H) 1842 cm^{-1} (br).

(3) Thermal Decomposition Studies. (a) Pyrolysis of 1. The weight changes by TGA started at 120 °C. Two severely overlapping weight loss stages between 120 and 230 °C were observed with a total weight loss of 55.5%. No additional weight loss occurred up to 500 °C. Calculated weight change for: $[H_2GaP(SiMe_3)_2]_3 = 3GaP + 6HSiMe_3$, 59.6%. A sample of **1** [0.23 g (0.31 mmol)] was pyrolyzed in a sublimator under vacuum at 200 °C for 2 h and at 450 °C for 3 h with the collection of volatiles. Small amounts of a viscous liquid were observed to condense on colder parts of the apparatus (confirmed to be $P(SiMe_3)_3$ by NMR) and the main product was a black solid, 0.12 g (theoretical 0.10 g). EA: Ga, 61.26; P, 27.16; Si, 5.59; C, 1.00; H, 0.48; Ga/P = 1.0/1.0; P/Si = 4.4/1.0; C/Si = 0.4/1.0. Noncondensables (CH_4 and H_2), approximately 0.65 mmol (0.01 g); condensables ($HSiMe_3$), 0.95 mmol (0.07 g). Weight of volatiles, approximately 0.08 g. An XRD pattern for the black product matched JCPDS file 12-191 for cubic GaP; average particle size, 2.3 nm. Another sample of **1** was pyrolyzed under vacuum at 400 °C for 2 h and at 600 °C for 0.5 h, and an XRD pattern for the black product matched JCPDS file 12-191 for cubic GaP; average particle size, 29.4 nm.

(b) Pyrolysis of the Toluene-Insoluble Solid. Continuous weight changes by TGA for the orange product from the reaction in toluene commenced at 30 °C with most losses occurring in the 100−200 °C range, 20%, and smaller losses to 400 °C, 3%; total weight change to 500 °C, 23%. In another experiment, 0.38 g of the orange solid was placed in a sublimer that was attached to a −196 °C cold trap. The system was briefly evacuated and then closed under static vacuum. The sublimer was heated at 200 °C for 2 h and at 475 °C for 3 h with the collection of volatiles. Some brown solid deposited on the colder parts. The final product was a shiny black solid, 0.22 g or weight loss of 0.16 g. EA: Ga, 64.76; P, 28.69; Si, 2.64; C, 3.53; H, 0.79; Ga/P = 1.0/1.0; P/Si = 9.9/1.0; C/Si = 3.1/1.0. Noncondensables (CH_4 and possible H_2), approximately 0.8 mmol (0.01 g); condensables ($HSiMe_3$), 1.8 mmol or 0.13 g. Weight of volatiles, 0.14 g. An XRD pattern for the black product matched JCPDS file 12-191 for cubic GaP; average particle size, 5.1 nm.

Reaction System $H_3Ga{\cdot}NMe_3/As(SiMe_3)_3$. (1) Synthesis of $[H_2GaAs(SiMe_3)_2]_3$ (2) in Et_2O. A sample of freshly prepared $H_3Ga{\cdot}NMe_3$ (0.40 g, 3.0 mmol) was dissolved in 20 mL of Et_2O. To this, a solution of $As(SiMe_3)_3$ (0.88 g, 3.0 mmol) in 20 mL of Et_2O was added at room temperature. After being stirred overnight, the yellow solution was concentrated to 5−10 mL and stored at −30 °C. After 1 to 2 days, the solution darkened and some colorless crystals appeared, 0.21 g (24% based on eq 1 (vide infra)). X-ray quality crystals were obtained at −30 °C from the ethereal solution of **2** after separating freshly formed crystals from the mother liquor. If the crystals were left in the liquor at −30 °C or higher temperatures, they would soon disappear, the solution acquiring an orange color, and a yellow-orange solid precipitating. Also, increased concentrations of the reactants accelerated the formation of the insoluble product. For crystals, melting behavior: 130−150 °C, change of color to black; no melting to 300 °C. Anal. Found (calcd) for $C_{18}H_{60}Ga_3As_3Si_6$: C, 24.37 (24.59); H, 6.68 (6.88). ^{1}H NMR: δ 0.49 (54H, $SiMe_3$), 4.65 (6H, GaH_2, br). $^{13}C\{^1H\}$ NMR: δ 2.15. MS. *m*/*e* (intensity)(ion): peak clusters around 877 (3)($[H_2GaAs(SiMe_3)_2]_3$ − H or M − H), 805 (3)(M − $SiMe_3$), 791 (2)(M − $SiMe_3$ − Me + H), 731 (1)(M − $2SiMe_3$ − H), 657 (83)(M − $3SiMe_3$ − 2H or M − $As(SiMe_3)_2$), 586 (100)($[H_2GaAs(SiMe_3)_2]_2$ or M*), 512 (100)(M* − $SiMe_3$ − H), 497 (11)(M* − $SiMe_3$ − Me − H), 363 (10)(M* − $As(SiMe_3)_2$ − 2H or M* − $3SiMe_3$ − 4H), 291 (100)($H_2GaAs(SiMe_3)_2$ − H or M** − H), 222 (93)($HAs(SiMe_3)_2$), 206 (56)($As(SiMe_3)_2$ − Me), 191 (11)($As(SiMe_3)_2$ − 2Me), 134 (31)($HAsSiMe_2$), 73 (100)($SiMe_3$), 69 (4)(Ga), 59 (32)($HSiMe_2$). IR: ν(Ga−H) 1834 cm^{-1}.

(2) Reaction of $H_3Ga{\cdot}NMe_3$ with $As(SiMe_3)_3$ in Toluene. The reaction in toluene was performed similarly as above. Coloration of the solution with concurrent formation of colorless crystals were observed at −30 °C 1 day past addition, as in the Et_2O reaction system. Upon concentrating the mixture to approximately 10 mL, a yellow-orange insoluble solid formed and no crystals were observed anymore. After one week of storage at −30 °C, the volatiles were removed affording an orange solid. EA: Ga, 29.29; As, 36.79; C, 19.39; H, 4.84; Ga/As = 0.9/1.0; H/C = 3.0/1.0; C/As = 3.3/1.0. ^{1}H and $^{13}C\{^1H\}$ NMR spectra for a toluene-d_8 slurry of the solid showed peaks for $As(SiMe_3)_3$, $HSiMe_3$, and H_2 and a weak, very broad feature at δ 0.7. IR: ν(Ga−H) 1830 cm^{-1} (br).

(3) Thermal Decomposition Studies. Pyrolysis of the Toluene-Insoluble Solid. A TGA curve for the orange solid isolated one week after addition (as above) showed two stages for weight changes: 30−250 °C, 13% and 250−500 °C, 9%; total weight loss, 22%. For pyrolysis, 0.32 g of the orange solid was placed in a sublimer that was attached to a −196 °C cold trap. The system was briefly evacuated and closed under static vacuum. The sublimer was heated at 200 °C for 2 h and at 475 °C for 3 h, and volatiles were collected. Some orange-brown solid deposited on the colder parts. The final product was a black solid, 0.20 g, or weight loss of 0.12 g. EA: Ga, 48.23; As, 34.26; Si, 3.03; C, 0.23; H, 0.12; Ga/As = 1.5/1.0; As/Si = 4.2/1.0. Noncondensables (CH_4 and possible H_2), approximately 0.5 mmol (0.008 g); condensables ($HSiMe_3$), 1.1 mmol (0.081 g). Weight of volatiles, 0.09 g. An XRD pattern for the black product matched JCPDS file 14-450 for cubic GaAs; average particle size, 3.4 nm. In another experiment, some of the orange solid was refluxed in xylenes (bp 137−144 °C) for 40 h. Soon after the beginning of reflux, the solid turned dark brown-black. Upon completion, the dark solid was dried under vacuum. An IR spectrum for the solid contained some weak vibrations for CH_3 groups but no Ga−H stretches. An XRD spectrum showed two broad halos at 2Θ 28° and 49° that were consistent with the onset of GaAs crystallinity.

Structural Analyses of 1 and 2. Suitable colorless crystals of **1** and **2** were sealed in glass capillaries. Specimens of **2** were stored at −30 °C prior to determinations and a locally designed low-temperature transfer device was used to keep the sample cold (<−40 °C) during its removal from the capillary and subsequent transfer to the goniometer. For **1**, systematic absences in the data and diffraction symmetry

Table 2. Selected Bond Distances (Å) and Angles (deg) for **1** and **2** with Estimated Standard Deviations in Parentheses

1		**2**	
		Bond Lengths	
P(1)−Ga(1)	2.387(2)	As(1)−Ga(1)	2.4752(8)
P(1)−Ga(1B)	2.397(2)	As(1)−Ga(3)	2.4695(8)
		As(2)−Ga(1)	2.4717(9)
		As(2)−Ga(2)	2.4733(8)
		As(3)−Ga(2)	2.4831(8)
		As(3)−Ga(3)	2.4721(8)
Ga(1)−H(4)	1.50 (assumed)	Ga(1)−H(1)	1.50(3)
		Ga(1)−H(2)	1.49(3)
P−Si	2.267(3)	As−Si(av)	2.355
		As−Si; min/max	2.349(2)/2.361(2)
Si−C (av)	1.827	Si−C (av)	1.857
Si−C; min/max	1.810(12)/1.847(9)	Si−C; min/max	1.847(7)/1.868(7)
		Bond Angles	
Ga(1B)-P(1)−Ga(1)	126.35(10)	Ga(3)−As(1)−Ga(1)	127.99(3)
		Ga(3)−As(3)−Ga(2)	126.57(3)
		Ga(1)−As(2)−Ga(2)	126.69(3)
P(1A)-Ga(1)−P(1)	113.65(10)	As(2)−Ga(1)−As(1)	111.76(3)
		As(2)−Ga(2)−As(3)	110.64(3)
		As(1)−Ga(3)−As(3)	110.49(3)
H(4)−Ga(1)−H(4A)	107.7 (assumed)	H(2)−Ga(1)−H(1)	132(4)
		H(4)−Ga(2)−H(3)	129(4)
		H(6)−Ga(3)−H(5)	121(4)
Si(1B)−P(1)−Si(1)	107.9(2)	Si(2)−As(1)−Si(1)	108.74(7)
		Si(4)−As(2)−Si(3)	105.95(8)
		Si(6)−As(3)−Si(5)	107.91(7)
		H(2)−Ga(1)−As(2)	97(3)
H(4)−Ga(1)−P(1)	108.8	H(2)−Ga(1)−As(1)	95(3)
		H(1)−Ga(1)−As(2)	117(3)
		H(1)−Ga(1)−As(1)	102(3)
		Torsion Angles	
		Ga(2)−As(2)−Ga(1)−As(1)	−2.19(6)
		Ga(1)−As(2)−Ga(2)−As(3)	−16.38(6)
		Ga(1)−As(1)−Ga(3)−As(3)	−4.86(6)

indicated any of the hexagonal space groups $P6_3$, $P6_3/m$, and $P6_322$. E-statistics strongly favored the centrosymmetric alternative, $P6_3/m$, which proved to be correct on the basis of the results of refinement. For **2**, systematic absences and intensity statistics determined the space group $P2_1/n$. The structures were solved by direct methods. All non-hydrogen atoms were refined with anisotropic displacement parameters. For **1**, all hydrogen atoms were placed in ideal positions and refined as riding atoms with relative isotropic displacement parameters. In the case of **2**, the C hydrogens were treated as above, but the Ga hydrogens were all located from the difference map and were refined isotropically; the Ga−H bond lengths were constrained to be similar to each other by using the SHELXL constraint SADI. Details of the data collection for **1** and **2** are summarized in Table 1, and Table 2 contains selected bond distances and angles.

Acknowledgment. R.L.W. thanks the Office of Naval Research for its financial support.

Supporting Information Available: Crystal packing diagrams for **1** and **2**; tables of bond distances, bond and torsion angles, anisotropic temperature factor parameters, and atomic fractional coordinates for **1** and **2** (12 pages). See any current masthead page for ordering and Internet access instructions.

JA9731837